13th Int Symp on Applications of Laser Techniques to Fluid Mechanics
Lisbon, Portugal, 26-29 June
Paper #1134

Measurement of Universal Velocity Profile in a Turbulent Channel Flow with a Fiber-Optic Profile Sensor

Katsuaki Shirai[1], Christian Bayer[1], Thorsten Pfister[1], Lars Büttner[1], Jürgen Czarske[1], Harald Müller[2], Gentaro Yamanaka[3], Hermann Lienhart[3], Stefan Becker[3], Franz Durst[3]

1: Department of Electrical Engineering and Information Technology, Dresden University of Technology, Dresden, Germany, Email: shirai@iee.et.tu-dresden.de, Internet: http://eeemp1.et.tu-dresden.de
2: Department 1.4 Gas Flow, Physikalisch-Technische Bundesanstalt, Braunschweig, Germany
3. Institute of Fluid Mechanics, Friedrich-Alexander-University Erlangen-Nürnberg, Cauerstr. 4, 91058 Erlangen, Germany

Abstract The near-wall velocity measurement of the boundary layer in a turbulent channel flow was conducted through glass plates attached flush to the wall. For high spatially resolved measurements, different types of laser-Doppler velocity-profile sensors were developed based on two different techniques. One sensor system was based on the use of two different wavelengths for distinguishing two fringe systems. The other sensor system utilized only a single wavelength but two different carrier frequencies. Preliminary to the flow measurements the effect of the glass plates for optical access was estimated and the vibration of the wind tunnel was investigated. The insertion of a glass plate shifts the location of the measurement volume. As long as the sensor is traversed perpendicular to the plate, this shift remained constant and the calibration curve doesn't vary. This fact ensures the applicability of the velocity-profile sensor to internal flows with optical access windows. It turned out that some care should be taken for the vibration effect of the tunnel itself when the profile sensor is used with a high spatial resolution. The flow measurements were conducted by two sensors with three different conditions of Reynolds number and glass plate. The measured mean and fluctuating velocity distributions were scaled well with the wall variables. They also showed good agreement with available DNS data of fully developed channel flow. It was found that sufficiently large samples are required to make reliable estimation of turbulent statistics with high spatial resolution. The results demonstrate the feasibility of the sensor to be applied to turbulent flow research with its advantageous high spatial resolution.

1. Introduction

In turbulent flow there is a wide range of different temporal and spatial scales involved with the energy transfer from large to small scales. In order to investigate phenomena of interest, the choice of measurement technique with an appropriate resolution becomes crucially important with respect to temporal and spatial scales. Flow measurement with insufficient resolution gives biased results and leads to the wrong interpretation of the phenomena. The lack of temporal resolution induces the aliasing effect on the high frequency turbulence fluctuation. Measurement with an insufficient spatial resolution hinders from resolving small-scaled motions compared to the size of the measurement volume.

Among optical velocity measurement techniques for turbulent flow, laser Doppler anemometry (LDA) and particle image velocimetry (PIV) are the ones which are used in most cases. Both techniques are based on particles which trace the flow to be measured. LDA offers one-point measurement with relatively high spatial and temporal resolution. The use of multiple pairs of beams enables multiple component measurement of velocity in a single point with a finite dimension. On the other hand, PIV offers two-dimensional measurement of velocity in the plane with moderate space and time resolution. The used of two cameras for observation enables the measurement of velocity in the out-of-plane direction, which enables three component velocity in a plane. In general, LDA gives higher spatial and temporal resolution although it cannot give the information of turbulent structure due to the point nature of the measurement technique. Recently, the use of high speed CMOS camera has enabled PIV measurement on the order of 10 kHz (Tanahashi et al., 2004). The advent of micro PIV has made it possible to measure micro scaled flow with a spatial resolution of micrometer range (Santiago et al., 1998, Meinhart et al., 1999). Although the main application has been confined in the field of microfluidics, however, its potential to turbulent flow research is sought by Kähler et al (2005).

Considering the temporal and spatial resolution of particle-based optical flow measurement techniques, the temporal resolution depends on the rate of tracer particle flowing through the control volume. An excessive rate of tracer particles in the control volume at the same time makes problem of signal processing. However, in general, the higher the seeding concentration, the higher the temporal resolution can be achieved. On the other hand, the spatial resolution of particle-based optical measurement techniques is ultimately dependent on the size of the tracer particles. For high speed flow tracer particles with smaller diameter should be used to avoid the failure of the particles to follow the flow although the scattering optical power decreases with smaller size particles. The spatial resolution is generally determined by the size of the control volume. The smaller the volume, the higher the spatial resolution is achieved. However, the smaller size of the control volume reduces the particle rate flowing through the volume. It is known that the insufficient spatial resolution makes small-scaled motions to be spatially averaged inside the dimension of the volume.

Laser-Doppler velocity-profile sensor is a velocity measurement technique to solve the spatial averaging effect of conventional LDAs (Czarske 2001, Czarske et al., 2002). The sensor utilizes two fringe systems inside the measurement volume and it resolves the position as well as the velocity of single tracer particles inside the volume. The main advantage of the sensor is its high spatial resolution compared to conventional LDAs without reducing the size of the measurement volume. Hence, high spatially resolved velocity measurement is achieved without reducing the data rate. The sensor is expected to be applied to turbulent flow research especially with high Reynolds number flow, where the small scale of turbulence becomes smaller. However, there have not been reported many applications which demonstrates the feasibility of the sensor to turbulent flow research.

This paper reports on an application of novel laser-Doppler velocity-profile sensors to turbulent flow research. The purpose of this report is to demonstrate the applicability of the profile sensor to a canonical turbulent flow with a high spatial resolution. Velocity measurements with a high spatial resolution in a two-dimensional channel flow are reported. We have developed velocity-profile sensor systems based on two different techniques. The sensors were applied to three different conditions of Reynolds numbers through glass window mounted flush to the wall. The preliminarily investigation on the effect of the glass plate and the vibration of the wind tunnel were conducted. The measured mean and fluctuating velocity profiles shows good agreements among different Reynolds number conditions and with DNS data.

2. Flow

The flow measurements were carried out in a two-dimensional channel flow at the Institute of Fluid Mechanics (LSTM) in the University of Erlangen-Nürnberg in Germany. As the details of the tunnel have already reported by Zanoun et al. (2003), only the overview is summarized here. The working fluid was air and the flow was tripped at the entrance to advance the transition to turbulence. The dimensions of the cross-sectional area were 600 x 50 mm. The flow was regarded as a two-dimensional flow from its aspect ratio of 12 (Dean, 1978). The measurement location was placed at the location where the flow was considered to be fully developed and was not affected by the open exit at the same time. The distance of the measurement location from the channel inlet was beyond about 6000 mm and it corresponded to 120 *H* (*H*: channel full width), which was considered to be sufficient for the fully developed condition of turbulent channel flow. At the measurement location, two glass plates (thickness: 6 mm) were mounted flush to the wall so that they function as the upper and the lower channel walls with optical access (Fig. 1). In one of the measurement configurations an optical glass plate with anti-reflection coating (thickness: 2 mm) was attached in one of the sides. The measurements were conducted with forward scattering configuration for better signal-to-noise ratio condition. For tracer particles, diethylhexyl-sebacate (DEHS) was seeded from the upstream of the blower of the wind tunnel.

The measurements were carried out with three different Reynolds number conditions. The Reynolds number was determined by the friction velocity and the channel half-width. The wall shear stress was important in the measurement of universal velocity profile, since the wall shear stress was used for non-dimensionalizing the coordinates through the friction velocity. Because of outlier points and the uncertainty of the absolute position of the measurement volume, we had a difficulty of obtaining reliable value of the wall shear stress from the slope of the mean velocity profile close to the wall (Shirai et al., 2006). This time the wall shear stress was independently estimated from the streamwise pressure gradient. The wall-static pressure was measured along the centerline of the channel in streamwise direction.

3. Velocity Profile Sensor

Laser-Doppler velocity-profile sensors based on two different techniques were used for the flow measurements. The principle of the profile sensor is briefly explained here and it is followed by the description of each sensor system. The principle is described in details in other papers (Czarske, 2001, Czarske et al., 2002).

3.1 Principle

The laser-Doppler velocity-profile sensor is based on the use of two light-interference fringe systems created at the measurement volume as shown in Fig. 2. Unlike a conventional LDA using a single pair of parallel fringe system, the profile sensor utilizes two pairs of fringe systems with different fringe spacing slopes. The Doppler frequencies obtained by a single scattering particle with velocity U can be given as

$$f_i = \frac{U}{d_i}, \qquad (1)$$

where f_i and d_i are Doppler frequency and fringe spacing in each channel (i=1, 2). If the spacings of the respective fringe systems has a slope in the optical axis (z-direction), the quotient of the Doppler frequencies generated by the two fringe systems becomes a function of z coordinate:

$$q(z) = \frac{f_2}{f_1} = \frac{U/d_2(z)}{U/d_1(z)} = \frac{d_1(z)}{d_2(z)}. \qquad (2)$$

Taking the inverse of the calibration curve Eq.(2) yields the position z when the fringe spacing variation is a monotonic function along the z-direction. The velocity is calculated through the Eq.(1) with using the measured Doppler frequency and the positional information determined from the Eq. (2). Hence, the position as well as the velocity of single particles passing through the measurement volume is determined if the fringe spacing variation is known through calibration. For distinguishing the two Doppler frequencies, one can use either different wavelengths (Czarske, 2001) or different carrier frequencies (Pfister et al, 2005). Note that the positional information does not depend on the particle velocity, which ensures the unambiguous measurement of position and velocity with a wide dynamic range. The spatial resolution depends on the steepness of the calibration function (Czarske et al., 2002). Since the sensor gives the positional information, the sensor has a spatial resolution inside the measurement volume and therefore high spatially resolved velocity measurement is enabled without traversing the measurement volume hundreds of times.

3.2 Sensor Systems

The present paper reports on the measurement results with two different systems of the profile sensor. One of the sensor systems is based on a wavelength-division-multiplexing (WDM) technique, in which two wavelengths are used for distinguishing two fringe systems created in the measurement volume. The other system utilized a frequency-division-multiplexing (FDM) technique, in which only one wavelength but two different carrier frequencies are used to distinguish the fringe systems.

The WDM sensor utilizes two laser diodes with wavelengths of 685 nm and 785 nm. The setup is shown in Fig. 3. The beams from the diodes were collinearly combined by a dichroic mirror and a diffractive grating was used as a beam splitter. The working distance was about 80 mm and the size of the measurement volume was about 500 μm. The scattering light was detected in the forward direction and it was separated into the two wavelengths with a dichroic mirror. Two Si photo-detectors were used and the data acquisition was carried out with a 2ch A/D converter installed in a computer. The basic setup of the optics is similar to the one reported in Czarske (2001) and Czarske et al. (2002) except for the use of a diffractive grating. The signal was detected with a specially developed software-based dynamic method, which was extended from the former processing program reported by Shirai et al. (2005). The dynamic signal detection is necessary for the profile sensor because of the wide dynamic range of velocity occurrence. It is due to the long measurement volume size in the direction of steep velocity gradient in the measurement of boundary layer in the case of a velocity-profile sensor. The WDM sensor is not equipped with a heterodyne technique for measuring the velocity close to zero, but the measurement of velocity close to zero about 0.1 m/s was possible with a specially developed algorithm based on the Gaussian shape of the envelope of a Doppler signal. Several validation conditions were used based on the signal-to-noise ratio and some other criteria, which will be reported in another occasion. A pinhole of 2 μm diameter attached on a rotating disk was used for calibrating the sensor. The rotational frequency of the disk was precisely controlled and it was attached on a precision linear stage for scanning the measurement volume. The spatial resolution and the relative accuracy of velocity measurement were experimentally estimated to be 1.5 μm and 0.06 %.

The FDM sensor utilizes a single wavelength but two carrier frequencies. The beam from a single mode laser with output power of 150 mW was split into four beams. Three of them were frequency shifted to 120, 80 and 60 MHz with acousto-optic modulators (AOMs). Each of the four beams was coupled into a single mode (SM) fiber and delivered to the measurement head. The beams were aligned in an alternate way to create two carrier frequency pairs of 120 MHz and 20 MHz (Fig. 4). The measurement volume was created at about 300 mm distance from the head. The dimensions of the measurement volume were about 100 x 100 x 900 μm. The scattering light detected with a forward direction was coupled into a single Si photo-detector. The electrical output from the detector was split and they were down-mixed with the corresponding carrier frequencies (Fig. 5). Since the reference frequencies from the AOMs were used for the down-mixing, the effect of the frequency drift of the AOMs was successfully avoided. The down-mixed signals were acquired with a 2ch A/D board installed in a computer. Same procedures of the signal processing and the calibration as it was used for the WDM sensor were used for the FDM sensor. The details of the system are described in Pfister et al. (2005). The spatial resolution and the relative accuracy of velocity measurement were estimated to be 6 μm and 0.085 %.

4. Measurement Conditions

The measurement conditions and specification of the sensors are summarized in Table 1. Empirical equations by Dean (1978) are used for estimating the Reynolds number Re_B (based on the channel full-width) and bulk mean velocity U_B. The sample points shown in the Table 1 are the number of the validated samples in the measurements. The spatial resolution and the relative accuracy of velocity measurement were experimentally evaluated with the glass plate inserted between the measurement head and the measurement volume.

Table 1. The details of the three measurement conditions (l_x x l_y x l_z: measurement volume size, Δz: spatial resolution, $\Delta U/U$: relative velocity measurement accuracy, T_{glass}: glass plate thickness, Re_τ: Reynolds number based on friction velocity and channel full-width, l_τ: viscous length)

sensor type	l_x x l_y x l_z [μm]	Δz [μm]	$\Delta U/U$ [%]	T_{glass} [mm]	Re_τ	Re_B	U_B [m/s]	l_τ [μm]	sampled points
WDM	100 x 100 x 500	1.5	0.06	2	420	14000	4.5	60	21444
WDM	100 x 100 x 350	6	0.06	6	780	30000	9.2	32	8984
FDM	100 x 100 x 900	6	0.085	6	1100	44000	16.0	23	35179

The flow measurements were conducted with three different Reynolds number conditions: two measurements with the WDM sensor and one with FDM sensor. The first case (Re_τ=420 with the WDM sensor) was chosen in order to see the ability of the sensor to measure the data close to the wall. The difference of the first case and the second case (Re_τ=780 with the WDM sensor) was the different material and thickness of glass plates as well as Reynolds number conditions. Especially, the thickness of the glass plate was expected to give an effect on the WDM sensors due to the chromatic aberration which refracts the lights with different wavelengths toward different angles. However, it turned out that the thickness was not critical for the present WDM sensor because of the relatively small difference of the wavelengths used for the sensor. The thick glass plate reduced the size of the measurement volume, which was not due to the effect of the thickness but the signal quality smeared by the glass. The effect of thicker glass plate and the glass-plate quality should be further investigated. In this point the FDM sensor may have an advantage with less aberration effects due to the use of single wavelength especially when a thick glass window is used. The FDM sensor was applied for a moderately high Reynolds number condition.

The streamwise wall-pressure gradients measured along the channel centerline are shown in Fig. 9. The linear behavior of the pressure drop indicates that the flow was fully developed by the measurement location (x = 6 m). From the linear slope of the pressure gradient the wall shear stress was estimated based on the force-balance equation between the pressure gradient and the wall shear stress.

Before each measurement, calibration of the sensor was carried out with a glass plate with the same material and thickness used in the flow measurement in order to compensate the effect of the glass plate. The effect of the glass plate inserted between the measurement head and the measurement location is shown in Fig. 7 in a preliminary experiment. In Fig. 7 the calibration curve with and without glass plate is plotted. The “position 1” and “position 2” means that the glass plate was placed at different positions between the measurement head and the measurement volume. The insertion of the glass plate indeed shifts the calibration curve in the optical axis direction as can be seen in Fig. 7. Besides, the effective size of the measurement volume is decreased for the case of the 6mm thick glass plate with the WDM sensor. However, with the glass plate the calibration curve doesn't change with respect to the position of the plate because the sending beams are equally refracted by the glass plate. Hence, a single calibration is sufficient to conduct measurements with a velocity profile-sensor as long as the sensor is traversed perpendicular to the wall.

Before the flow measurements, the vibration of the wind tunnel was measured by varying the tunnel velocity. A triangulation sensor (resolution of 0.1 μm) was used to measure the deflection of the wind-tunnel wall close to the measurement location. The sensor was attached to a frame which was independent from the wind tunnel in order to avoid the vibration to be transferred to the triangulation sensor due to the contact. The vibration showed an increased amplitude as the wind tunnel speed was increased. The results indicated that the tunnel had a maximum vibration amplitude of about 35 μm at the flow of Re_τ=1100 in the experimental conditions.

For obtaining the statistics one can use a slot technique either with constant width or constant samples in each slot. In either case the statistics are calculated in each slot, which is necessary for the velocity-profile sensor since it resolves the position of the velocity. The slot technique has to make averages within the slot, however, sufficiently dense data samples would yield statistically reliable data with much higher spatial resolution compared to conventional LDA. The choice of slot width and slot samples with a finite number of total data points has a trade-off relationship with the statistical accuracy in each slot. In addition to the validation conditions in the signal processing, an outlier reduction scheme was used to eliminate outlier points which could not be reduced through the validation conditions. The scheme is based on the linear fit of the data in each slot (Fig. 8). It can be assumed that the trend of the data (velocity gradient) varies linearly inside the slot as long as the slot width is taken sufficiently small. Besides, the velocity distribution at each small slot was assumed to be Gaussian distributed. The standard deviation calculated with the data in the slot is used as a cut-off reference for the outlier reduction. The data outside *m*-times the standard deviation with linear trend were regarded as outliers and reduced. This procedure was repeated until no more outlier was found in each slot. For the reduction, the value of m=4 was used throughout the data analysis.

5. Measurement Results and Discussion

The raw velocity profiles obtained in the measurements are shown in Fig. 9. Each of the points in the plots corresponds to single Doppler bursts. The mean and the fluctuating velocity normalized with wall variables are plotted in Fig. 10 and 11. For the results shown in the figures, the constant-width slot technique with 50 % overlap of the slot was applied to avoid the abrupt change of the statistics from slot to slot for each set of the data. Slot width was fixed for each data set but varied for data taken at different conditions by checking the statistical convergence of data in the slots. The slot width was increased for the fluctuating velocity since the higher order central moment needs more samples to be convergent. For comparison, an available direct-numerical-simulation (DNS) data in a fully developed channel flow (Abe et al., 2001) is plotted together. The position of the wall was roughly estimated from the mean velocity close to the wall with an equal sample per slot technique and the equation suggested by Cenedese et al (1998). After that a slight adjustment was applied in order to avoid the strong effect of the wall-proximity points contaminated by remaining outliers. The measured mean velocity profiles show good agreement among them except the wall-proximity points, which was supposed to be contaminated with remaining outliers. However, the mean velocity measured at the case of Re_τ=420 shows a smooth behavior until close to the wall ($z^+ \approx 1$). The wall shear stress estimated from the near-wall data of Re_τ=420 was in an excellent agreement (within 3 %) with the one determined from the streamwise wall-pressure gradient. The measured profiles also show a good agreement with the DNS data. The fluctuating velocity profile (Fig. 11) shows fairly well scaled and the peak value shows a slight dependence on Reynolds number, but this is not clear whether it is from the flow itself or from the scattering of the data. The location of the peak is about z^+=15, which is also in a good agreement with other reported peak locations. However, the results still show some fluctuating behavior which is likely due to the insufficient number of samples per slot especially after the peak locations.

The authors tried to estimate the "universal" constants of the "logarithmic law-of-the-wall" from the measurement data, but it was not successful due to the relatively small numbers of samples taken in the measurements with limited duration. The inherent low probability of particles which comes into the near-wall region have to be overcome for taking large samples in a limited measurement duration. Larger amount of statistically independent data would provide more reliable statistics up to higher order moments with high spatial resolution.

6. Concluding Summary

We have developed laser-Doppler velocity-profile sensors and reported its application to the measurements in a turbulent boundary layer flow. The sensors are based on the wavelength-division-multiplexing (WDM) and frequency-division-multiplexing (FDM) technique. The sensors were characterized with respect to the spatial resolution and the velocity measurement accuracy. The flow measurements were conducted in a fully developed channel flow with Reynolds numbers of Re_τ = 420, 780 and 1160 with the different sensors through glass window attached flush to the wall. The effects of the glass window and the vibration of the wind tunnel were evaluated before the experiments. The results indicated that the glass window shifts the measurement volume as in the case of a conventional LDA. However, it was demonstrated that the measurement with traversing the sensor is possible without any serious problem as long as the sensor is traversed perpendicular to the wall. The vibration effect of the wind tunnel turned out to be close to the spatial resolution of the sensor, therefore care should be taken for the vibration and the deflection of the wind tunnel during the measurement and the data analysis. For the measurements a refined signal processing technique was developed and an additional new outlier reduction scheme was applied to the flow measurement results. The measured mean and fluctuating velocity distributions showed good agreements among the three measurements. They also had a good agreement with a DNS data with moderate Reynolds number in a channel flow. One of the measurement results showed an excellent agreement of the wall shear stress estimated from the near-wall data and independently measured by streamwise pressure gradient. These facts demonstrate the feasibility of the velocity-profile sensor to turbulent flow research, especially to the investigation of small scaled structures in high Reynolds number conditions where a non-intrusive measurement technique with high spatial resolution is needed. The estimation of the universal constants for the logarithmic law-of-the-wall was tried, but it turned out that the number of samples were not sufficient to make a reliable statement on it. It was due to the low data rate and the processing time for the software-based burst detection technique used for the present sensors in a limited duration of the measurements.

In the future work, sufficiently large data sample is required for calculating reliable turbulent statistics with high spatial resolution. The use of offline processing or hardware based signal processing might help this point. The detection of signals with backward-scatter mode will be tested for severe applications with a single optical access. The sensors are to be applied to challenging applications in turbulent flows. Two-point lateral spatial correlation statistics and particle acceleration will be measured with high spatial resolution.

Acknowledgements

The authors acknowledge Mr. A. Voigt for his work on the FDM sensor. The support from the

Deutsche Forschungsgemeinschaft (DFG) is highly appreciated (CZ55/18-1).

References

Abe H, Kawamura H, Matsuo Y (2001) Direct numerical simulation of a fully developed turbulent channel flow with respect to Reynolds number dependence. ASME J Fluids Eng 123:382-393

Cenedese A, Romano GP, Antonia RA (1998) A comment on the “linear” law of the wall for fully developed turbulent channel flow. Exp Fluids 25: 165-170

Czarske J (2001) Laser Doppler velocity profile sensor using a chromatic coding. Meas Sci Technol 12: 52–57

Czarske J, Büttner L, Razik T, Müller H (2002) Boundary layer velocity measurements by a laser Doppler profile sensor with micrometre spatial resolution. Meas Sci Technol 13: 1979–1989

Dean RB (1978) Reynolds number dependence of skin friction and other bulk flow variables in two-dimensional rectangular duct flow. ASME J Fluids Eng 100: 215–223

Kähler CJ, McKenna R, Scholz U (2005) Wall-shear-stress measurements at moderate Re-numbers with single pixel resolution using long distance Micro-PIV - an accuracy assessment, 6th International Symposium on Particle Image Velocimetry, September 21-23, Psadena, California, USA

Meinhart CD, Wereley ST, Santiago JG (1999) Piv Measurements in a Microchannel Flow, Exp. Fluids 27: 414-419

Pfister T, Büttner L, Shirai K, Czarske J (2005) Monochromatic heterodyne fiber-optic profile sensor for spatially resolved velocity measurements with frequency division multiplexing. Appl Opt 44: 2501–2510

Santiago JG, Wereley ST, Meinhart CD, Beebee BJ, Adrian RJ (1998) A PIV System for Microfluidics, Exp. Fluids 25: 316-319

Shirai K, Pfister T, Czarske J (2005) Signal processing technique for boundary-layer measurements with a laser-Doppler velocity- profile-sensor. In: Proceedings of the 13th international symposium GALA-Fachtagung: Lasermethoden in der Strömungsmesstechnik, 6–8 September 2005, Cottbus, Germany, pp 4.1–4.8

Shirai K, Pfister T, Büttner L, Czarske J, Müller H, Becker S, Lienhart H, Durst F (2006) Highly spatially resolved velocity measurements of a turbulent channel flow by a fiber-optic heterodyne laser-Doppler velocity-profile sensor, Exp. Fluids 40: 473–481

Tanahashi M, Fukuchi Y, Choi GM, Fukuzato K, Miyauchi T (2004) The time-resolved stereoscopic digital particle image velocimetry up to 26.7 kHz, International Symposium on Applications of Laser Techniques to Fluid Mechanics, July 12-15, Lisbon, Portugal, Session 8.1

Zanoun ES, Durst F, Nagib H (2003) Evaluating the law of the wall in two-dimensional fully developed turbulent channel flows. Phys Fluids 15: 3079–3089

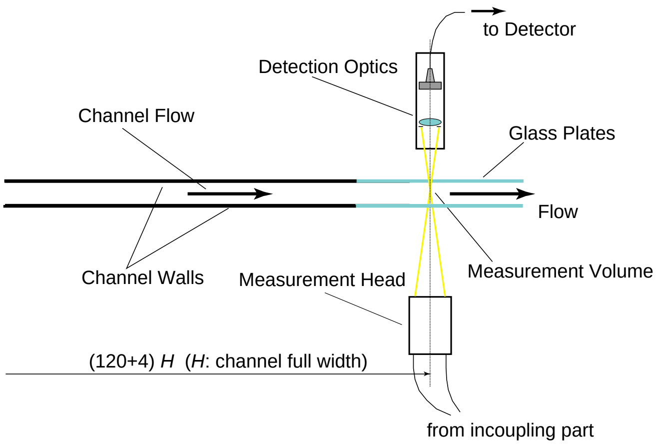

Fig. 1 The measurement configuration of the two-dimensional turbulent channel flow. The measurements were carried out through the glass plates mounted flush to the wall.

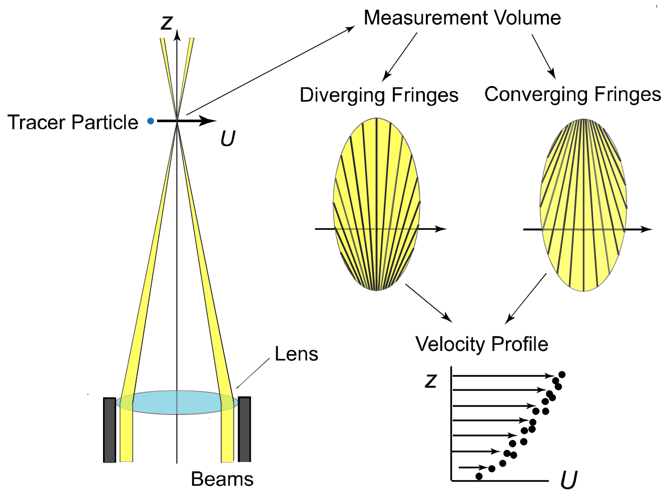

Fig. 2 The schematic explanation of the laser-Doppler velocity-profile sensor. The use of two fringe systems with different fringe slopes enables unambiguous determination of position as well as velocity of single tracer particles.

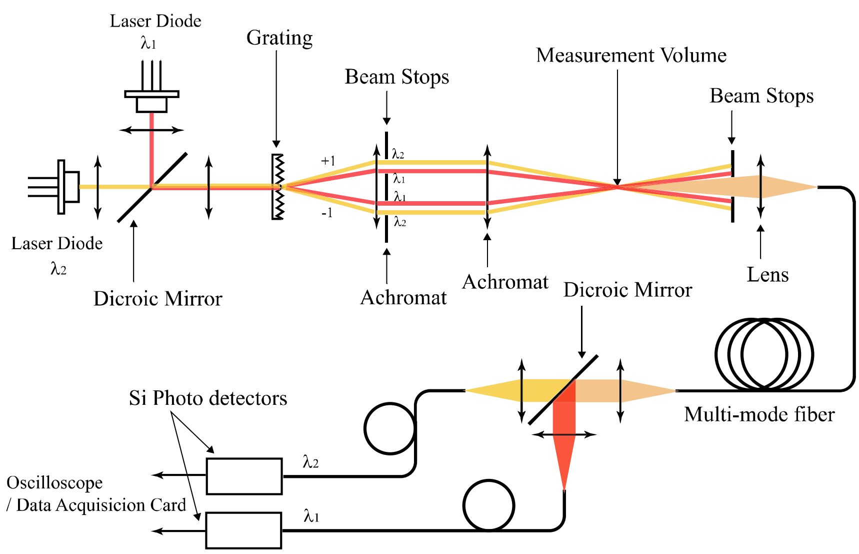

Fig. 3 The setup of the WDM sensor. Two wavelengths are utilized for distinguishing the two fringe systems. A grating is used as a beam splitter.

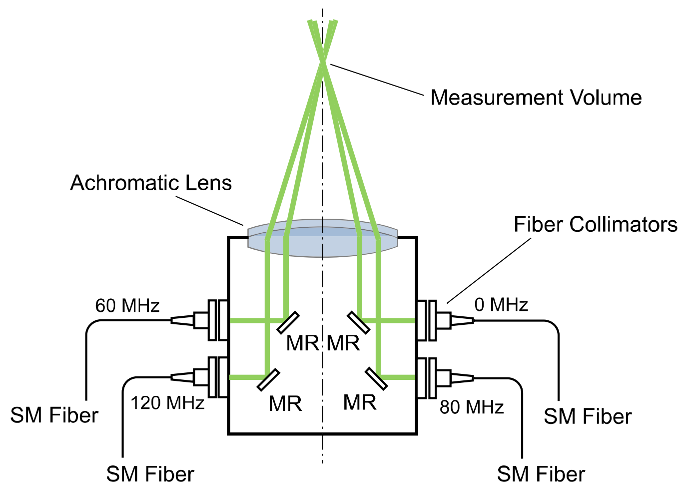

Fig. 4 The optical configuration at the measurement head of the FDM sensor. (SM fiber: single mode fiber, MR: mirror) The FDM sensor utilizes a single wavelength but two different carrier frequencies to distinguish two fringe systems.

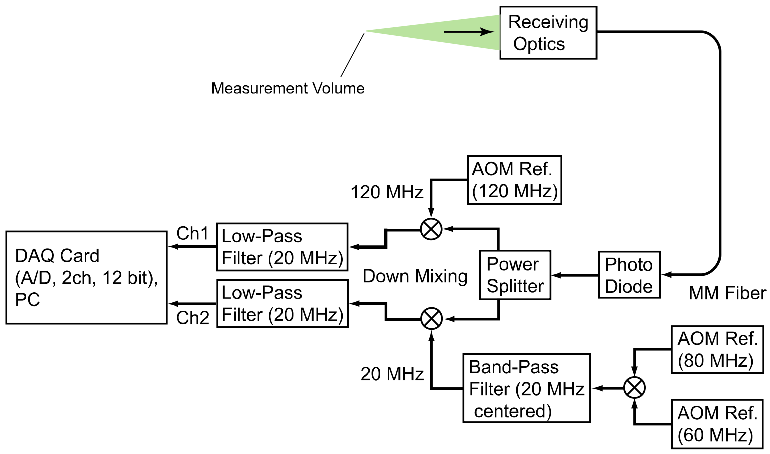

Fig. 5 Detection and signal processing part of the FDM sensor. The frequency drift is suppressed by using down-mixing with reference frequency of AOM drivers.

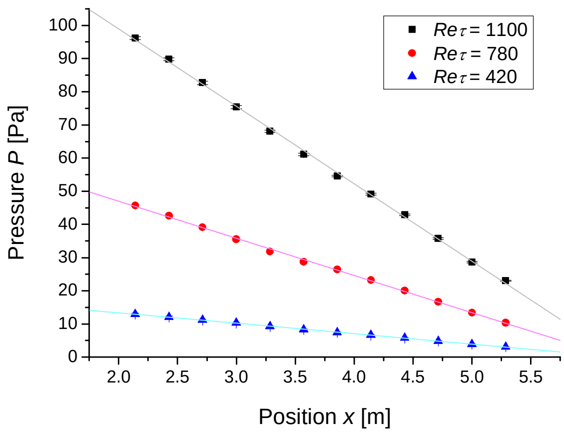

Fig. 6 Pressure drop in the streamwise direction at three measurement conditions (Reynolds number is based on the friction velocity and the half-width of the channel)

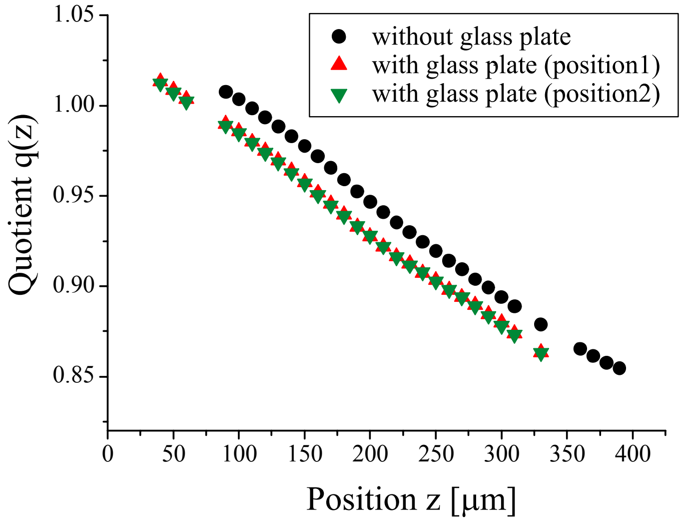

Fig. 7 Calibration curve obtained with a FDM sensor through 6 mm thick glass plate. Note that the curve is shifted parallel to the plate but the slope of the curve does not change when the position of the measurement volume was changed.

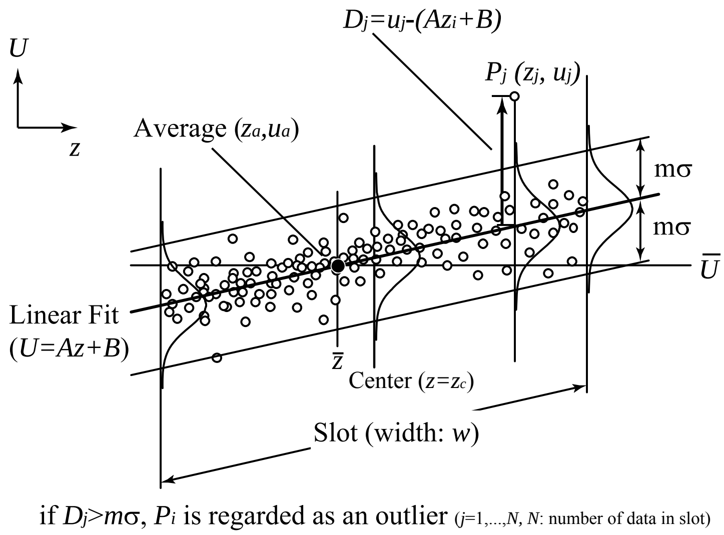

Fig. 8 Concept of linear-fit based data reduction scheme. The data inside a slot is examined based on the linear fit to the data in each slot. The data outside the *m*-times standard deviation from the linear trend is regarded as outliers and discarded.

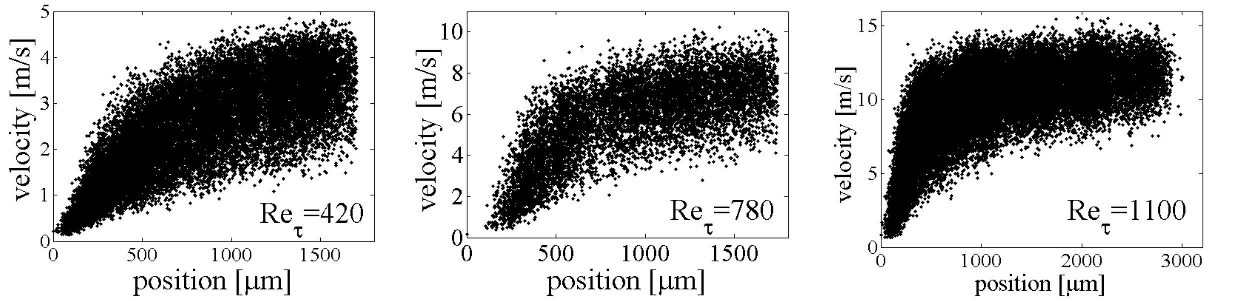

Fig. 9 Raw data plot of the velocity profiles after validation for the three measurement conditions. Each points represents single Doppler burst pairs.

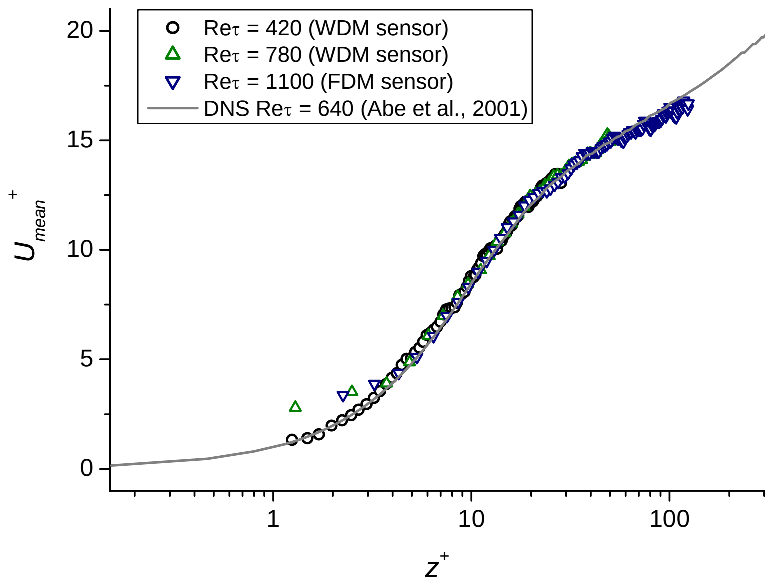

Fig. 10 Measured mean velocity profile compared with DNS data (Abe et al., 2001). The coordinates are normalized with wall variables.

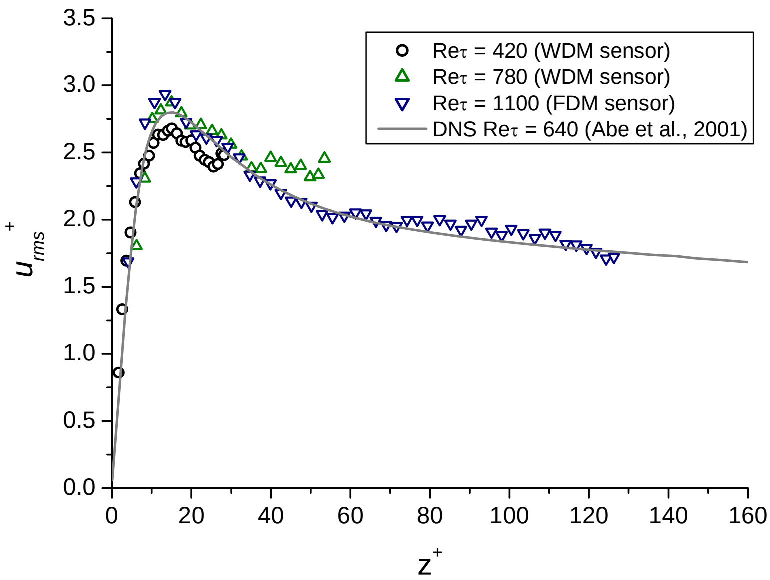

Fig. 11 Measured fluctuating velocity profile compared with DNS data (Abe et al., 2001). The coordinates are normalized with wall variables.